Effect of local skin blood flow during light and medium activities on local skin temperature predictions

Journal of Thermal Biology 84 (2019) 439–450

Contents lists available at ScienceDirect

Journal of Thermal Biology

journal homepage: www.elsevier.com/locate/jtherbio

Effect of local skin blood flow during light and medium activities on local skin temperature predictions

Stephanie Veselá[a,*], Boris R.M. Kingma[a,b], Arjan J.H. Frijns[a], Wouter D. van Marken Lichtenbelt[c]

[a] Department of Mechanical Engineering, Eindhoven University of Technology, the Netherlands
[b] TNO, The Netherlands Organization for Applied Scientific Research, Unit Defense, Safety & Security, Soesterberg, the Netherlands
[c] Dept. of Nutrition and Movement Sciences, NUTRIM School of Nutrition and Translational Research in Metabolism of Maastricht University Medical Center, the Netherlands

ARTICLE INFO

Keywords:
Thermoregulation
Local skin blood flow
Mathematical modelling
Local skin temperature

ABSTRACT

The quality of local skin temperature prediction by thermophysiological models depends on the local skin blood flow (SBF) control functions. These equations were derived for low activity levels ($0.8 - 1\ met$) and mostly in sitting or supine position. This study validates and discusses the prediction of foot SBF during activities of $1 - 3\ met$ in male and females, and the effect on the foot skin temperature prediction ($\Delta T_{skin,foot}$) using the thermophysiological simulation model ThermoSEM. The SBF at the foot was measured for ten male and ten female human subjects at baseline and during three activities (sitting, walking at $1\ km/h$, preferred walking around $3\ km/h$). Additional measurements included the energy expenditure, local skin temperatures ($T_{skin,loc}$), environmental conditions and body composition. Measured, normalized foot SBF is 2-8 times higher than the simulated SBF during walking sessions. Also, SBF increases are significantly higher in females vs. males (preferred walking: 4.8 ± 1.5 versus 2.7 ± 1.4, $P < 0.05$). The quality of $\Delta T_{skin,foot}$ using the simulated foot SBF is poor (median deviation is $-4.8°C$, maximumum deviation is $-6°C$). Using the measured SBF in ThermoSEM results in an improved local skin temperature prediction (new maximum deviation is $-3.3°C$). From these data a new SBF model was developed that includes the walking activity level and gender, and improves SBF prediction and $\Delta T_{skin,foot}$ of the thermophysiological model. Accurate SBF and local skin temperature predictions are beneficial in optimizing thermal comfort simulations in the built environment, and might also be applied in sport science or patient's temperature management.

1. Introduction

The international energy agency reports that space heating and cooling as well as water heating are responsible for almost 55% of the global buildings energy use. Moreover, the report states that the energy consumption of these sectors needs to be reduced by at least 25% by 2050 to meet the 2 °C target for climate global warming (IEA, 2013). However, heating, ventilation and air conditioning systems should also provide a healthy and comfortable thermal indoor environment for the buildings' occupants. Among other solutions, localized heating and cooling systems show a high potential for saving energy in office buildings as compared to conventional systems while providing a comfortable indoor thermal environment (Arens et al., 1991; Foda and Sirén, 2012; Melikov et al., 1994; Verhaart et al., 2015; Veselý and Zeiler, 2014). To predict the overall and local thermal sensation and comfort of the users of these systems efficiently, human thermophysiological models and coupled thermal sensation models can be used. Therefore, thermophysiological models such as UTCI-Fiala (Fiala et al., 2012, 2001, 1999), ThermoSEM (Kingma, 2012; Kingma et al., 2014; Severens, 2008; Severens et al., 2007), Berkeley Comfort Model (Huizenga et al., 2001; Zhang et al., 2001) or Tanabe's model (Tanabe et al., 2002) predict the mean and local skin temperatures, which are then processed in thermal sensation and comfort models. Because of their main application in the built environment, these models are designed and validated for mild cold to mild warm environmental conditions (approximately 15 °C to 35 °C, depending on clothing). Within this environmental temperature range, the prediction of mean and local skin temperatures need to be as accurate as possible. Validations of thermophysiological models show high accuracies for mean skin temperatures, but deviations can be found in local skin temperatures

Abbreviations: BMI, Body mass index; BMR, Basal metabolic rate; EE, Energy expenditure; LDF, Laser Doppler Flowmetry; MRUM, Metabolic Research Unit Maastricht University; SBF, Skin blood flow; SD, Standard deviation; SE, Standard error; ThermoSEM, Thermophysiological Simulation model Eindhoven Maastricht

* Corresponding author.
E-mail address: steffi.vesela@gmail.com (S. Veselá).

https://doi.org/10.1016/j.jtherbio.2019.07.033
Received 9 April 2019; Received in revised form 16 July 2019; Accepted 27 July 2019
Available online 29 July 2019

especially at the extremities (Martínez et al., 2016; Psikuta et al., 2012; van Marken Lichtenbelt et al., 2007; Veselá et al., 2015). To improve the prediction of local skin temperatures, influencing factors of the local heat balances in these models need to be re-evaluated.

One important component of these balances is the local skin blood flow (SBF), which is a large thermoregulatory factor (Kellogg, 2006). Local SBF is mainly controlled via the nervous system of warm and cold sensitive neurons at the skin sites and in the hypothalamus (Boulant, 2005). Depending on the fire rate of these thermosensitive neurons, SBF will be reduced or elevated through vasoconstriction or vasodilation to avoid or increase heat loss, respectively (Mekjavič and Morrison, 1985; Nakamura and Morrison, 2008a, 2008b). The modelling of local SBF can be done using different approaches, for example Wissler's or Fiala's empirical SBF models (Fiala et al., 2001; Wissler, 2008), the SBF model by Tanabe where the SBF is a function of the external work and shivering heat production (Tanabe et al., 2002), Pennes' empirical blood flow perfusion term in the Berkley Comfort model (Huizenga et al., 2001; Pennes, 1948) and the neurophysiological approach by Kingma et al. (2014). The validation of the neurophysiological approach by Kingma et al. (2014), which was implemented in the thermo-physiological model ThermoSEM, showed improved forearm and abdomen SBF and mean skin temperature prediction.

ThermoSEM including the neurophysiological approach for SBF was developed and validated for several environmental conditions. However, the activity levels were low at $0.8 - 1$ *met* for most scenarios and in sitting or supine position with low clothing insulation (Kingma et al., 2014). Higher activity levels such as standing (about 1.5 *met*) or walking ($2 - 4$ *met*) were not included in the model's validation. In the most recent thermophysiological models, the overall activity level is used to take different activities into account (Fiala et al., 2001; Huizenga et al., 2001; Tanabe et al., 2002). However, during activities, like walking, a local increase in muscle activity/metabolism takes place, but also a large increase in local blood perfusion is observed (Hinds et al., 2004; Joyner et al., 2001; Savard et al., 1988; Snell et al., 1987). Yet, data on local (increased) metabolic rates and local increase in blood perfusion during activities is lacking or incomplete (Veselá et al., 2017a). Moreover, most models use an average, usually male, person for simulation purposes. Havenith (2001) and van Marken Lichtenbelt et al. (2004) show that the individual body characteristics of human subjects, such as height, body mass, body fat percentage and metabolism, improve the models quality in predicting individual skin temperatures. Our final aim is to extend the thermophysiological model ThermoSEM such that it includes both localized increase in tissue perfusion and local increase in metabolic rates that depend on the type of activity. In the present paper, our focus was on the local increase in blood perfusion and its effect on the increase in local skin temperatures. The main focus was hereby on the foot, since the largest deviations of up to $10°C$ in skin temperature between simulation and measurements were found at this body location (Veselá et al., 2015).

To verify and improve the foot skin temperature prediction of ThermoSEM for light and medium activity levels as usually found in the built environment (sitting, standing, walking at about $2 - 3$ km/h), the influence of the SBF at the ankle is investigated. Therefore, local skin temperatures and ankle SBF of twenty human subjects were measured for activities reaching from $1 - 3$ *met* for this study. The main objective was to investigate the effect of the measured SBF on local skin temperature prediction based on individual characteristics in the thermophysiological simulation model ThermoSEM. Moreover, the influence of walking activity level and gender was included in the neurophysiological approach.

2. Methods

2.1. Human subject experiments

The experiments were conducted at the Metabolic Research Unit of Maastricht University (MRUM) and took place from February to August 2016. The experiments described in this paper were part of a larger study investigating the thermal challenges of modern day humans. The medical ethical committee of Maastricht University Medical Centre + authorized the experimental protocol. All participants in this study signed a letter of consent prior to the experiments.

Table 1
Participants characteristics (10 males, 9 females).

Characteristics	Mean (± SD) - all	Mean (± SD) - male	Mean (± SD) - female	P-values male vs. female
Age [yr]	28.7 ± 10.6	30.2 ± 11.0	26.1 ± 9.7	0.44
Body mass [kg]	69.4 ± 9.4	75.2 ± 8.7	63.1 ± 4.9	< 0.01
Height [m]	1.76 ± 0.08	1.81 ± 0.06	1.71 ± 0.06	< 0.01
BMI [kg/m^2]	22.3 ± 2.4	22.9 ± 2.7	21.7 ± 1.7	0.28
Body fat [%] [a]	24.7 ± 7.0	21.9 ± 8.1	27.9 ± 3.3	0.06
Surface area [m^2] [b]	1.85 ± 0.15	1.95 ± 0.12	1.74 ± 0.08	< 0.01

[a] Measured via Bod Pod®.
[b] Method by Du Bois and Du Bois (1916).

2.1.1. Subjects

The subjects had to meet the following inclusion criteria: Caucasian, generally healthy, age between 18 and 60 years, BMI of $20 - 25$ kg/m^2 and sharing an office with another participant of different gender. The last criterion was required for the wider study. Hence, ten pairs of male-female volunteers were recruited for this study (Table 1). One female subject was excluded from the analysis, because no skin perfusion of the ankle was recorded due to a malfunction of the LDF probe. As shown in Table 1, there is a significant difference in body mass, height and body surface area between the male and female test persons.

2.1.2. Measurement protocol

The recruited volunteers visited MRUM for one day. The chamber's air temperature was set to $22\,°C$ and was recorded using hygrochron iButton® dataloggers (DS1923, Maxim Integrated, USA) at four heights ($0.1m$, $0.6\,m$, $1.1m$, $1.7\,m$ above ground) along with the relative humidity (RH in %). The participants were asked to refrain from caffeine or alcoholic beverages and food up to 12 h before the start of the experiments. After arriving at 8:30 a.m., the subjects swallowed a small telemetric temperature pill (CorTemp™, USA), before they changed into the standardized medium warm clothing combination consisting of underwear, a t-shirt, a sweater, sweatpants, socks and sneakers (total insulation about 0.8 *clo*, see also section 2.2.3 and Table S1). While dressing, thermochron iButton® dataloggers (DS1922L, Maxim Integrated, USA) were attached on the test persons with medical tape on 14 positions plus on fingertip in accordance to EN-ISO 9886, 2004 (2004) as shown in Fig. S1, supplementary information. Furthermore, skin perfusion was measured using Laser Doppler Flowmetry (LDF) (PF4000 & PF5000, Perimed AB, Sweden). For practical reasons, the participants were wearing regular footwear, and to avoid distortion of the regular walking patterns, the SBF was measured at the ankles instead of the feet or toes.

With the sensors attached, the volunteers then performed the measurement protocol as shown in Fig. 1. Firstly, they laid in supine position on a stretcher for 30 min to measure baseline metabolic rate (BMR). To ensure that the participants' thermal state was close to neutrality, they were covered with a thin cotton blanket. Energy expenditure (EE) was measured during all parts of the experiments by indirect calorimetry using a mask connected to an automated respiratory gas analyser. After the BMR measurement, the subjects were given a light breakfast and changed into either the light clothing combination consisting of underwear, a t-shirt, shorts, socks and sneakers (total insulation about 0.5 clo) or left on the medium clothing combination (0.8 *clo*, see section 2.2.3 and Table S1). The starting

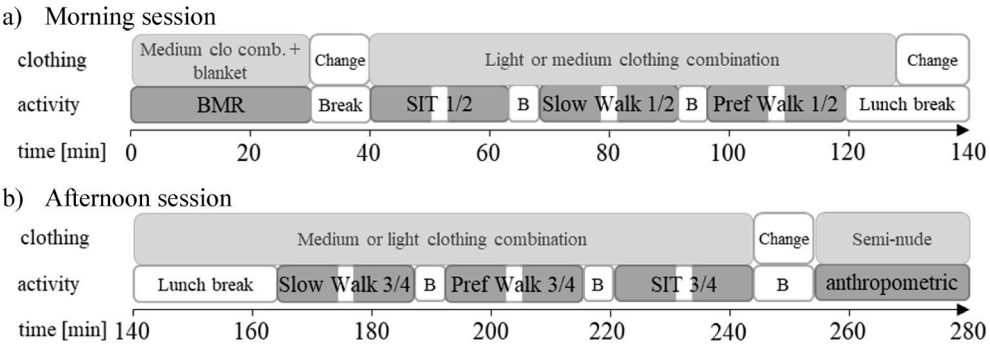

Fig. 1. Time line of measurement protocol. Light gray areas represent times of defined clothing, dark gray areas represent times of defined activities, white areas represent any kind of break (B) for taking measurements, changing clothing or eating and drinking. (The notation 1/2 and 3/4 refer to the two parts of each experimental session divided by a small break for taking measurements in the morning and afternoon, respectively.).

clothing combination (light or medium) was randomized for all pairs of subjects. Then, they switched to a treadmill where three activities took place for a total 23 min each (Fig. 1a). After the first 10 min of each activity, there was a small break (approximately 3 min) to perform additional measurements, e.g. blood pressure, and thermal comfort questionnaires (not evaluated in this paper). Because of this small break, all activities were split into two subsections, which are separated by the small white line in Fig. 1 and are numbered for further analysis 1/2 for the morning and 3/4 for the afternoon session. The activities were sitting on a chair, walking at a speed of 1 km/h (Slow Walk) and walking at preferred speed (Pref Walk). The slow walking period replaced a period of standing, which was found to be too hard on the participants in pretests. Hence, the walking speed was set to the lowest possible setting of the treadmills. In between the activities, the test persons could take off the EE mask for a couple of minutes and get a drink of water. The third activity was followed by a lunch break of 45 min. A light, standardized lunch of cheese and crackers was provided to the subjects. Also, the participants were asked to change into the second clothing combination. After the lunch break, the subjects performed the same three activities as before (Fig. 1b). However, due to technical reasons the seated period had to be performed as the final session. After the experiments, all sensors were detached and the volunteers' anthropometric data was measured. These data included the height, body mass, and body composition via Bod Pod® (Life Measurement Inc., Concord CA, USA).

2.2. ThermoSEM and input parameters

The thermophysiological model ThermoSEM was evolved from Fiala's thermoregulation model (Fiala, 1998; Fiala et al., 1999) with modifications implemented by Severens et al. (2007) and Kingma et al. (2014). In ThermoSEM, the human body is divided into 19 body parts which are represented by 18 concentric cylinders and one concentric semi-sphere. Each part consists of multiple tissue layers, e.g. bone, muscle, fat or skin, with a specific geometry and characteristics. The biggest difference between Fiala's model and the current version of ThermoSEM is the implementation of a neurophysiological approach to calculate the SBF (Kingma et al., 2014). The skin perfusion in Fiala's model is a function of the central stimuli for vasodilation and vasoconstriction which in turn are functions of the difference between the actual and set point mean skin temperature (Fiala, 1998; Fiala et al., 1999). The model by Kingma et al. (2014) formulates SBF regulation as:

$$\beta_i = \beta_{i,bas} \times N \times Q_{10} \quad (1)$$

where $\beta_{i,bas}$ is the basal heat equivalent of SBF of a specific body part i, Q_{10} is the local regulation effect of SBF (Q_{10}-effect) with $Q_{10} = 2^{\frac{(T_i - T_{i,bas})}{10}}$, $T_{i,bas}$ the local tissue temperature under basal conditions and N is the neural regulation signal for SBF. The function for N is:

$$N = \max[0, \gamma_1 - \gamma_2(H_{warm} - P_{cold}) - \gamma_3(H_{warm} - P_{warm})] \quad (2)$$

where γ_1 is a model constant representing all non-thermal effects on SBF, γ_2 and γ_3 are model parameters for the cold and warm afferent pathway, respectively, H_{warm} is the neuron fire rate of temperature sensitive neurons in the hypothalamus, P_{cold} and P_{warm} are the neural peripheral cold and warm drive, respectively. The function for the neural regulation signal is based on the neural concepts described in Mekjavič and Morrison (1985), Boulant (2005) as well as Nakamura and Morrison (2008a, 2008b). H_{warm}, P_{cold} and P_{warm} are calculated as described in Kingma et al. (2014) using the individual neuronal response characteristics as modelled by Mekjavič and Morrison (1985).

The SBF prediction using the neurophysiological approach was validated using two independent data sets of young male subjects, which were dressed in shorts or light sportswear and were lying in supine position (Kingma et al., 2014). The results of this validation showed improved SBF prediction as compared to Fiala's model for abdomen, forearm and similar SBF simulation for the hand. However, the model was not validated for higher activities and higher clothing insulation.

2.2.1. Individualized ThermoSEM

In the default setting, ThermoSEM represents an average adult male (73.5 kg, body surface area of 1.86 m^2, body fat percentage of 14%, and 87.1W total basal metabolic heat). However, the default geometry of ThermoSEM does not represent the participants of this study. Especially, a large deviation in the fat percentage can be seen in Table 1. van Marken Lichtenbelt et al. (2007) and Severens (2008, 2007) introduced a method to scale the default geometry of ThermoSEM to individual measurement. Firstly, the length of all body parts, except the head, were scaled with a factor λ_1 which is the ratio of the height of the actual person h to the height of the standard person h_0. The head was scaled with $\sqrt{\lambda_1}$. Secondly, λ_2 and λ_3 were introduced for scaling the layer thicknesses (i.e. radii) of the body segments. The core and muscle layers were scaled with λ_2, and the fat layers were scaled with λ_3. The thickness of the inner and outer skin was not scaled. The factors λ_2 and λ_3 were then calculated using an optimization routine to match the total body mass and fat percentage of the considered subject.

The general scaling method of van Marken Lichtenbelt et al. (2007) and Severens (2008) was adopted for this study. Additionally, differences in fat distribution between males and females were considered. Fig. 2 shows the distribution of the local body fat for a typical male and a typical female subject as compared to the standard (Fiala/ThermoSEM) configuration (Wölki, 2017; Wölki and van Treeck, 2013). The data was obtained from body composition measurements of 190 male and 133 female test persons. To produce similar relations in ThermoSEM additional factors were applied to λ_3 (Table 2). The resulting body fat mass distribution of a lean male (1.80 m, 70.1 kg, 16.4% body fat), the average male and average female human subject of this study are also shown in Fig. 2. Most male and all female participants of our study had a higher body fat percentage than in (Wölki, 2017), which results in overall higher body fat mass for all body parts especially on the thorax and abdomen. However, the distribution of body fat mass shows a similar relation. Hence, the additional scaling factors of Table 2 are sufficient to account for differences in body fat distribution between

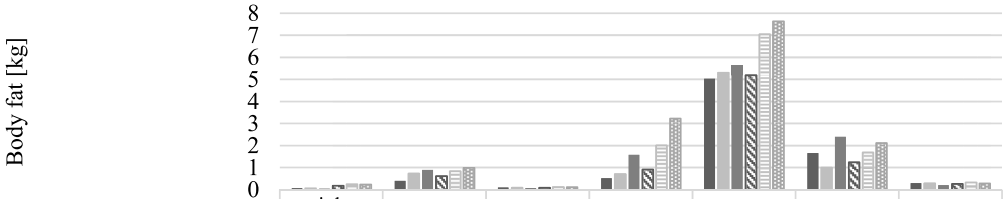

	right shoulder	right arm	right hand	thorax	abdomen	right leg	right foot
typical male subject *	0.07	0.40	0.10	0.52	5.03	1.65	0.29
std.Fiala FE*/ ThermoSEM	0.06	0.73	0.09	0.70	5.30	1.00	0.28
typical female subject*	0.05	0.90	0.07	1.58	5.63	2.40	0.21
study - lean male	0.18	0.61	0.09	0.92	5.19	1.24	0.26
study - avg male	0.24	0.83	0.12	2.01	7.05	1.69	0.32
study - avg female	0.24	0.99	0.11	3.23	7.64	2.12	0.29

Fig. 2. *Comparison of body fat mass distribution between the typical male subject, standard Fiala-FE/ThermoSEM and typical female subject of the study by Wölki (2017) (indicated by *) and this study's lean and average male and female subjects (Left body parts have the same value as right body parts.).*

Table 2
Adjusted scaling of the fat layer for male and female subjects.

Body part	Scaling factors	
	Male	Female
Face, Neck, Shoulders	λ_3	λ_3
Thorax	λ_3	$\lambda_3 \times 1.04$
Abdomen	λ_3	$\lambda_3 \times 1.02$
Upper arms	$\lambda_3 \times 0.98$	$\lambda_3 \times 1.05$
Lower arms	$\lambda_3 \times 0.98$	$\lambda_3 \times 0.99$
Upper legs	$\lambda_3 \times 1.05$	$\lambda_3 \times 1.14$
Lower legs	$\lambda_3 \times 0.999$	$\lambda_3 \times 0.99$
Hands, Feet	λ_3	λ_3

males and females in ThermoSEM.

2.2.2. Activity

If the activity is not constant, ThermoSEM requires an input file for the activity level at each time step t. In the model, the average activity during BMR measurements act_{BMR} is equal to 0.8 *met* (Fiala et al., 1999). The activity at each time point t (act_t) is then defined as the ratio of the energy expenditure at the time point t (EE_t) and the average metabolic rate during the BMR measurement (EE_{BMR}) times 0.8.

$$act_t = 0.8 \times \frac{EE_t}{EE_{BMR}} \tag{3}$$

Therefore, the measured data of the energy expenditure is averaged in 1 min intervals, and the average of the last 20 min during the BMR session is calculated. Because the energy expenditure could not be monitored during breaks, further assumptions had to be applied: 1) for longer breaks, the average metabolic rate of the first sitting session is used, 2) for short breaks during any walking sessions a linear decline to the first value, when the mask is put back on, is implemented.

2.2.3. Clothing

During the experiments, the volunteers wore a light and medium clothing combination. The light clothing ensemble consisted of underwear, shorts, a t-shirt, socks and sneakers. The medium ensemble included underwear, a t-shirt, a sweater, sweatpants, socks and sneakers. The t-shirt, shorts, sweater and sweatpants were provided for the subjects and were available in different sizes. The participants wore their own underwear and sneakers. The thermal clothing properties of both ensembles were measured at Empa, St. Gallen, Switzerland using the agile sweating thermal manikin SAM under two conditions: 1. the manikin was in stationary (non-moving), upright position and 2. the manikin was attached to the movement simulator and performed a walking motion of $2.5 km/h$. Details on the measurements can be found in Veselá et al. (2018, 2017b). The detailed local clothing area factor, intrinsic dry thermal insulation and clothing moisture permeability are given in Table S1 of the supplementary information. During BMR measurements, an additional cotton sheet was provided to ensure thermal neutrality. Since the additional clothing insulation provided by the cotton sheet could not be measured and no local values were found in the literature, an additional insulation of 0.07 m^2K/W was added based on whole-body covering items found in ISO 9920, (2009).

2.2.4. Environmental parameters

The environmental parameters required in ThermoSEM are the air temperature, radiative temperature, relative humidity and relative air speed. The air and radiative temperature as well as the relative humidity at each time step t is the average of the data provided by the four hygrochron iButtons (section 2.1.2). The average air temperature during the experiments was typically $24°C \pm 0.3°C$ and the relative humidity $30\% \pm 1\%$. The air speed was measured using a hot-wire thermal anemometer (FVA605TA10U, Ahlborn, Germany) and varied between 0.15 ms^{-1} and 0.20 ms^{-1}. These environmental conditions are prescribed to the model as described by Schellen et al. (2013).

2.2.5. Measured skin blood flow

To analyse the effect on local skin temperature prediction of measured SBF versus simulated SBF, the recorded perfusion response of the LDF measurement needed to be imported in ThermoSEM. However, using LDF for SBF measurements raises two issues: 1) Movement at the site of measurement, as is the case in the two walking modes, results in a Doppler shift associated with movement and not necessarily due to an increase in skin blood perfusion. Since LDF does not discriminate directionality of flow, summation of artifacts can result in large signal (Kirkpatrick et al., 1994), and 2) LDF does not provide absolute measurements of flow.

To estimate the SBF during walking without the movement artefacts, the 3 min of the LDF signal after the participants stopped walking were evaluated. Based on the study by Snell et al. (1987) and the assumption that the reduction in the LDF for the foot is similar to the leg SBF, we assume the mean of the 3 min directly after the movement should give a good estimation for SBF during the movement. Furthermore, the moving mean was used to reduce the noise of single peaks that occur during BMR, sitting or in the breaks between walking.

The resulting SBF signal cannot directly be used in ThermoSEM. However, the individual perfusion responses can be imported by normalizing the data based on the average value during BMR

measurement. In ThermoSEM, the normalized data is then converted into absolute values by multiplying the data with the averaged, simulated perfusion during the BMR phase. Similar to the EE, the perfusion could not be monitored during longer breaks. Since the subjects were mainly seated during the morning (after BMR) and lunch break, the averaged data of the first two sitting sessions was used to ensure a continuous data set.

2.2.6. Simulation

The simulation in ThermoSEM was done continuously covering the experimental boundary conditions from the beginning of the BMR measurements to the end of the last sitting session in 1 min time steps.

2.3. Data analysis

To summarize the data of the human subject experiments as well as the simulated results, the data was divided into the BMR measurement and 6 activity sessions: Sitting 1/2, Slow Walk 1/2, Pref Walk 1/2, Sitting 3/4, Slow Walk 3/4, Pref Walk 3/4. The data was averaged for each part of the 6 sessions over the last 5 min.

The measured and simulated activity levels and SBF are summarized for each session using Whisker-Box-Plots with outliers. An outlier is defined as a data point lying outside of 1.5 times the interquartile range and are displayed with a '+'. The mean values are marked with an 'x'.

Furthermore, a t-test was applied to the measured activity and SBF to see if there are any significant differences between the male and female subjects and the different activity levels. Similarly, the foot skin temperature difference was assessed. Beforehand, the data was tested for normality using the Shapiro-Wilk Original Test. For both tests, the significance level was set to $\alpha = 0.05$. The calculations were performed using the program Microsoft Excel.

To display the results on the effect of simulated versus measured local skin temperatures efficiently, the differences between these skin temperatures are shown.

3. Results

The averaged energy expenditure and activity level is presented in Fig. 3 and Fig. 4, respectively, using Whisker-Box-Plots for the male and female subjects separately. As expected, the energy expenditure and activity level increase with higher level of movement. In fact, the difference between increasing activity steps is significant in all cases for both, the energy expenditure and activity level (Table S2, supplementary information). Between the male and female participants, there are significant differences for the energy expenditure for all activities except the second preferred walking session. In fact, also for the first preferred walking sessions the p-value is close to the significance level $\alpha = 0.05$. This result is most probably due to the large variance of the energy expenditure data for this particular sessions. For the activity level (Fig. 4), no significant differences between male and female subjects are found.

3.1. Comparison of measured and simulated local skin temperatures

The averaged differences between simulated and measured core, mean skin and foot skin temperatures and their standard deviation of the 19 subjects are depicted in Fig. 5 for all 7 sessions in the order of performance. The results for the other body parts are included in the Supplementary Information Fig. S2 . For the average core temperature as well as mean, torso, arm, hand and leg skin temperature, the temperature difference is mostly close to $1°C$, which is within the expected measurement error of iButtons of $\pm\ 1°C$ (van Marken Lichtenbelt et al., 2006). However, the standard deviations reach values from 0.8 °C to $1.7°C$. The foot skin temperature differences ($\Delta T_{skin,foot}$) and their standard deviations have more extreme values, e.g. up to $6.0 \pm 2.4°C$ for the second preferred walking session. Even though $\Delta T_{skin,foot}$ is increasing over the day, there is no significant difference between stepwise increasing activity levels (Table S3, supplementary information). However, a significant difference between morning and afternoon sessions can be seen (Table S3). In the following sections, the influence of SBF on this finding is investigated. Further causes are debated in the discussion.

3.2. Measured versus simulated SBF

Fig. 6 shows examples of an LDF recording at the ankle for one male participant during the last 5 min of the subsessions BMR, sitting 2, and the last 5 min and subsequent 3 min of the subsessions slow walking 1 as well as preferred walking 1 and 3. The graphs of the other subsessions can be found in the supplementary information in Fig. S3. The LDF signal is very different for BMR and sitting sessions compared to walking sessions. During BMR and sitting, the signal is at one level with occasionally appearing larger peaks. For all walking sessions, it can be seen that the signal during walking is much higher than in the non-moving case with a high frequency of peaks and lows due to movement artefacts. The LDF signal after motion is stopped is similar to the one of the BMR and sitting session. For further analysis of all subjects, the moving mean of the LDF signal is used to reduce noise by occasional peaks and the values are normalized using the average of the BMR measurement.

The results for the normalized, measured foot SBF are summarized in Fig. 7. The mean values for the sitting session 1/2 and sitting session 3/4 are 0.7 and 0.9 for males and 1.2 and 1.7 for females, respectively. For both the male and female subjects, the normalized SBF increases for the slow walking session and again for the preferred walking session. This increase in SBF for increased, prescribed activity is significant (p-

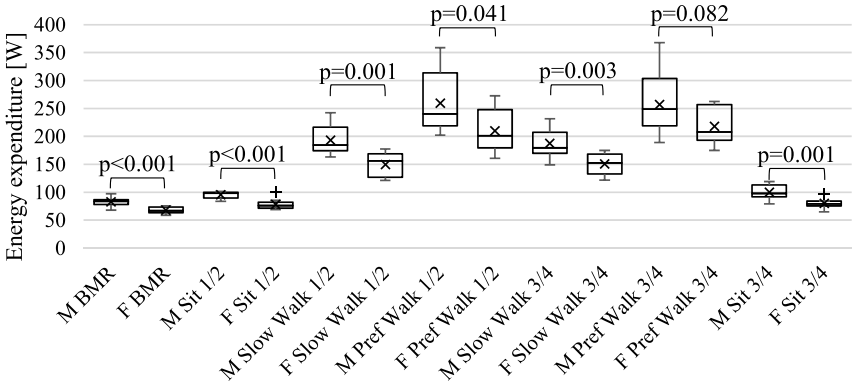

Fig. 3. Whisker-Box-Plot for average energy expenditure [W] of ten male (M) and nine female (F) subjects.

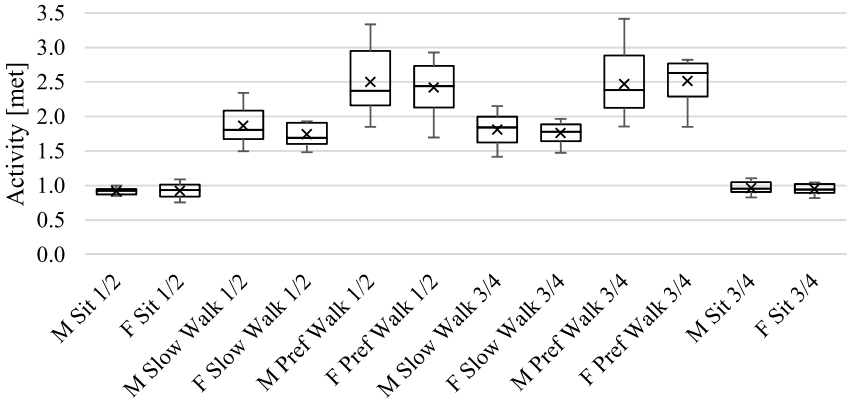

Fig. 4. Whisker-Box-Plot for average activity level [met] of ten male (M) and nine female (F) subjects as calculated in Eq. (3).

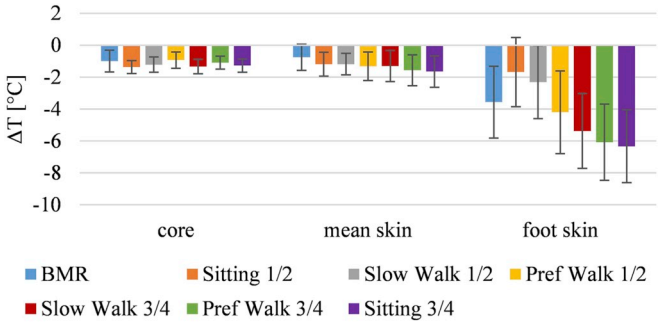

Fig. 5. Comparison of the core temperature, mean and foot skin temperature differences of all subjects (simulated - measured) using the standard SBF model (Kingma et al.) in ThermoSEM.

value < 0.05) for most performance steps (Table S4, supplementary information). However, for slow walking 3/4 to preferred walking 3/4 it is not significant (p-value of 0.09 for male and females), which is probably due to the large variations in between the subjects. In general, for the male subjects, the difference between the periods of slow walking and preferred walking is smaller than for the females. For all sessions, there is a significant difference ($\alpha = 0.05$) between the normalized foot SBF of the male and female participants (Fig. 7).

The normalized, simulated SBF for the default SBF settings (Kingma's neurophysiological model) and individual geometry in ThermoSEM are depicted in Fig. 8. The mean normalized, simulated foot SBF hardly differs for the sessions. Also, no differences can be found between male and female subjects. Moreover, the values are all below 1, which means that ThermoSEM predicts less SBF in the sessions with activity as compared to the basal situation.

All in all, the simulated foot SBF generally underestimate the measured foot SBF. The ratios of the mean normalized, measured SBF to the mean normalized, simulated SBF are summarized in Table 3. The magnitude for this underestimation corresponds to the activity level, but is different for male and female subjects. The ratio of the mean foot SBF of the walking sessions reaches values from 1.8 to 4.2 for males and 4.5 to 7.9 for females.

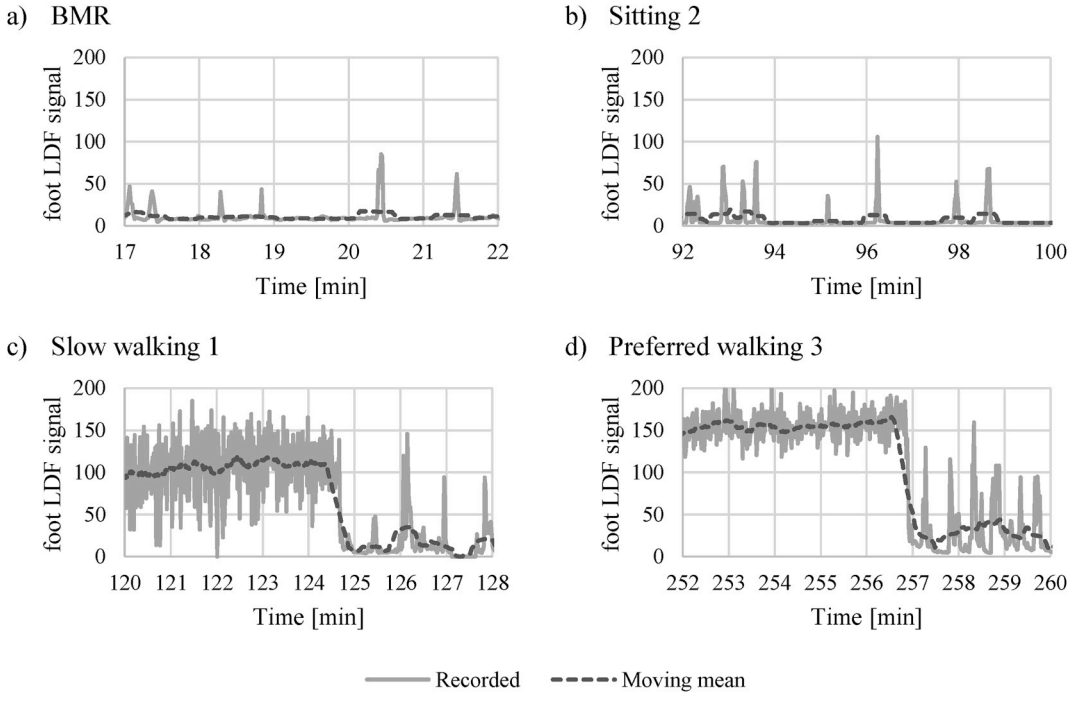

Fig. 6. Individual recording of LDF signal at the ankle and its moving mean.

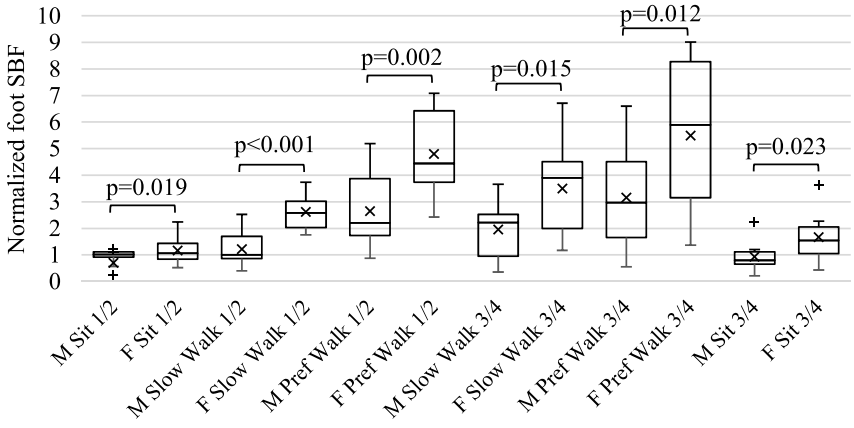

Fig. 7. Whisker-Box-Plots for normalized, measured foot SBF for ten male (M) and nine female (F) subjects with outliers (+).

3.3. Changes in skin temperature prediction for prescribed measured SBF

Fig. 9 and Fig. 10 compare simulation results for the difference in simulated and measured core, mean skin and foot skin temperatures ($\Delta T_{skin} = T_{skin.simulated} - T_{skin,\ measured}$) of the ThermoSEM simulation using a) the SBF for all body parts which is completely determined by the original thermoregulation model ThermoSEM (Kingma's neurophysiological model), named "original simulated SBF model" and b) the ThermoSEM model with the adjusted foot SBF, named "prescribed measured SBF model". The model is adjusted in such way that the computed SBF for the foot resembles the measured local SBF (see section 2.2.5). The results for the other body parts can be found in the supplementary information, Fig. S4.

Apart from the feet, $\Delta T_{skin,loc}$ is mostly the same for both simulations (Fig. 9 and Fig. S4). The core temperature difference is larger than the expected measurement error of $\pm$ 0.27 °C (Bongers et al., 2018) for the original and adjusted simulation with a mean difference of 1 °C to 1.3°C and a standard deviation for all subjects of 0.4°C to 0.7°C depending on the activity. The individual recording and simulation results as well as the individual residual mean squared deviation are shown in the supplementary information in Fig. S5, Fig. S6 and Table S5. A slight increase (about 0.05°C) can be seen for the simulation with the prescribed measured SBF. However, the difference of simulated minus measured core temperature is almost constant over the course of the simulation. Hence, on average the increase in core temperature due to activity is represented correctly by the simulation, even though the absolute values are not a precise representation of reality.

Running the adjusted ThermoSEM model lowers $\Delta T_{skin,foot}$ by about 1–2.7°C (Figs. 9 and 10). The standard deviation is mostly unchanged at 1.5 – 3°C. A slight difference can be seen between male and female foot ΔT_{skin} (Fig. 10). Especially, for female subjects, $\Delta T_{skin,foot}$ is overcompensated in the simulation with the prescribed, measured SBF resulting in positive values, which in absolute measures are sometimes higher than the original $\Delta T_{skin,foot}$. The significant difference between the morning and afternoon sessions for sitting and slow walking can be seen for both genders and in the original and adjusted simulation (Table S3, supplementary information). In fact, the magnitude of $\Delta T_{skin,foot}$ increases during the course of the day. Since this effect is not seen in other body parts, it might be due to the clothing of the foot during the experiments as will be elaborated in the discussion section.

3.4. Improvement of the model

The results in the previous sections show that (1) the normalized, simulated SBF is 2–8 times lower than compared to the normalized, measured SBF, (2) there is a significant difference in foot SBF between males and females, and (3) the local skin temperature prediction is improved by up to 3°C (new max deviation = 4°C), when the measured foot SBF serves as input data in ThermoSEM. To make the predictive SBF model also suitable for higher activity levels, there is a need to adjust the neurophysiological SBF model (equation (1) and (2)) by including the increase in activity level compared to BMR (0.8met), the gender of the simulated person and the interaction of these two parameters in equation (2). Therefore, an extended neural regulation signal N_{new} is introduced:

$$N_{new} = \max[0,\ \gamma_1 - \gamma_2(H_{warm} - P_{cold}) - \gamma_3(H_{warm} + P_{warm}) + \gamma_4 \cdot (act - 0.8) + \gamma_5 \cdot gen + \gamma_6 \cdot (act - 0.8) \cdot gen] \quad (4)$$

where (act – 0.8) is the increase activity level in met, gen represents the gender of the simulated person. For this study, the default gender is chosen to be "male" (gen = 0). The value for gender "female" is chosen to be gen = 1. The parameters γ_1 to γ_6 are the model's parameters to be

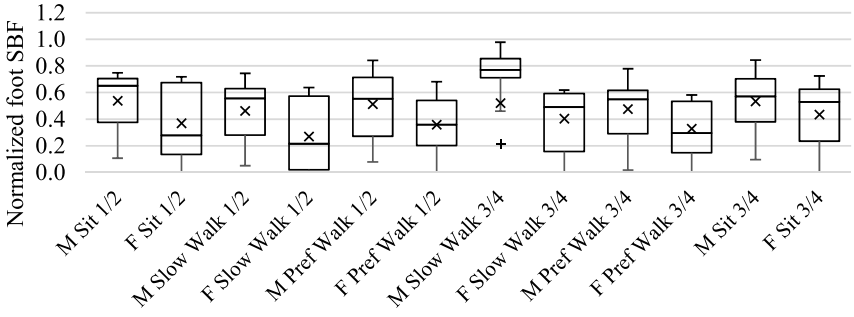

Fig. 8. Whisker-Box-Plots for normalized, simulated foot SBF for ten male (M) and nine female (F) subjects with outliers (+).

Table 3
Ratios of mean normalized, measured SBF and mean normalized, simulated SBF for the feet.

	M Sit 1/2	F Sit 1/2	M Slow Walk 1/2	F Slow Walk 1/2	M Pref Walk 1/2	F Pref Walk 1/2	M Slow Walk 3/4	F Slow Walk 3/4	M Pref Walk 3/4	F Pref Walk 3/4	M Sit 3/4	F Sit 3/4
$\frac{SBF_{norm,measured}}{SBF_{norm,simulated}}$	1.0	1.8	1.8	4.5	3.5	7.0	2.5	5.0	4.2	7.9	1.1	2.2

Fig. 9. Comparison of the core, mean skin and foot skin temperature differences of all subjects (simulated - measured) using the originally simulated SBF (shaded area) versus the prescribed measured SBF (filled area) in ThermoSEM.

determined for each body part.

As an example, the new neural regulation signal equation is determined for the foot using the k-fold cross validation scheme as described by Kingma et al. (2014). In this method, the coefficients γ_1 to γ_6 are iteratively fitted for n-1 subjects for n iterations, meaning that always one subject is left out at each iteration. Then, the root mean squared residual is calculated for the left-out subject. After all iterations, the n sets of coefficients are averaged. For the regression analysis, the measured, normalized foot SBF of this study had to be transferred to the equivalent absolute values in ThermoSEM (see section 2.2.5). Because of missing data points in core or skin temperatures for four subjects, which are needed to calculate H_{warm}, P_{cold} and P_{warm}, 15 subjects were included in the analysis. Moreover, the data was averaged over the last 5 min for each subsession (sitting 1, sitting 2, slow walking 1, etc.), resulting in 12 data points for each participant. Hence, the regression analysis included 180 data points. Furthermore, the

Table 4
Mean, standard error and ratio of mean and standard error of regression coefficients for the feet.

Coefficient	mean	SE	mean/SE
γ_1	3.5268	0.2392	14.7432[a]
γ_2	−0.1414	0.0111	−12.6956[a]
γ_3	0.3979	0.0323	12.3368[a]
γ_4	0.2873	0.0124	23.0798[a]
γ_5	−0.2085	0.0094	−22.1114[a]
γ_6	0.2573	0.0127	20.3262[a]

[a] = *|mean/SE| is above significance level (> 2.13).*

significance of the coefficients is tested using the t-statistics with a confidence level of 95%. The critical value of the t distribution is 2.13 for our data. Hence, the absolute value of the ratio of the mean of the fitted coefficients and the standard error SE should be larger than 2.13 for the parameters to be significant. In Table 4, the mean of the fitted coefficients, their standard error (SE), and the ratio of the coefficients mean and standard error for the feet are shown. All coefficients are significant for the regression equation. Hence, the SBF of the foot is estimated using the following equation for the neural regulation signal:

$$N_{new} = max[0,\ 3.5268 + 0.1414(H_{warm} + P_{warm}) - 0.3979(H_{warm} + P_{warm}) + 0.2873(act - 0.8) - 0.2085gen + 0.2573(act - 0.8)\cdot gen] \quad (5)$$

The simulations of the experiments were re-run using the new neurophysiological equation (5) for the foot SBF and the standard neurophysiological model (equation (2)) for all other body parts. The resulting $\Delta T_{skin,foot}$ using the new foot SBF equation, as shown in Fig. 11, has improved clearly for the male subjects. These values are similar to the situation where the measured foot SBF were explicitly prescribed in ThermoSEM. In fact, for the male participants a slight improvement (lower $\Delta T_{skin,foot}$) can be seen compared to the result from the measured SBF. For the female subjects, the foot skin temperature is now

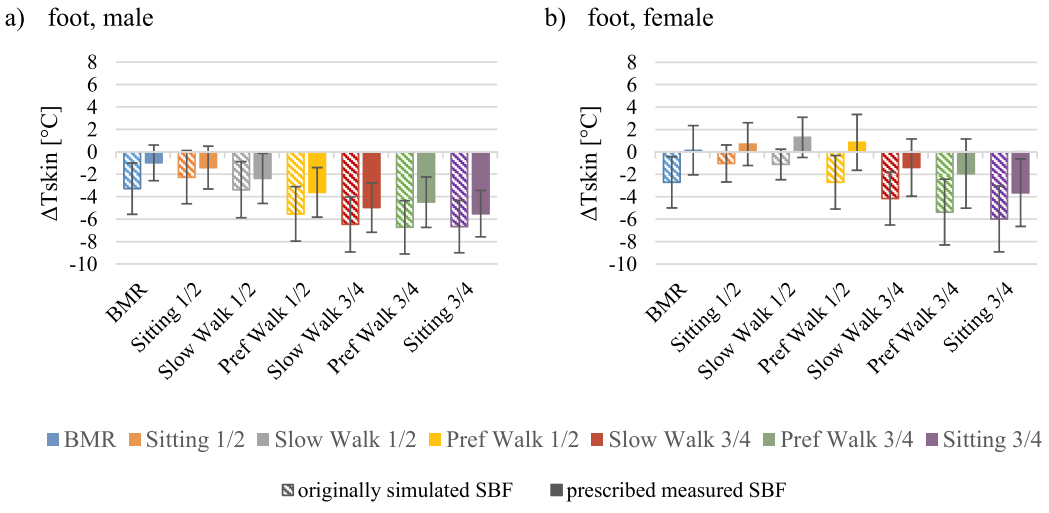

Fig. 10. Comparison of the local skin temperature differences of the foot for male and female subjects (simulated - measured) using the originally simulated SBF (shaded area) versus the prescribed measured SBF (filled area) in ThermoSEM.

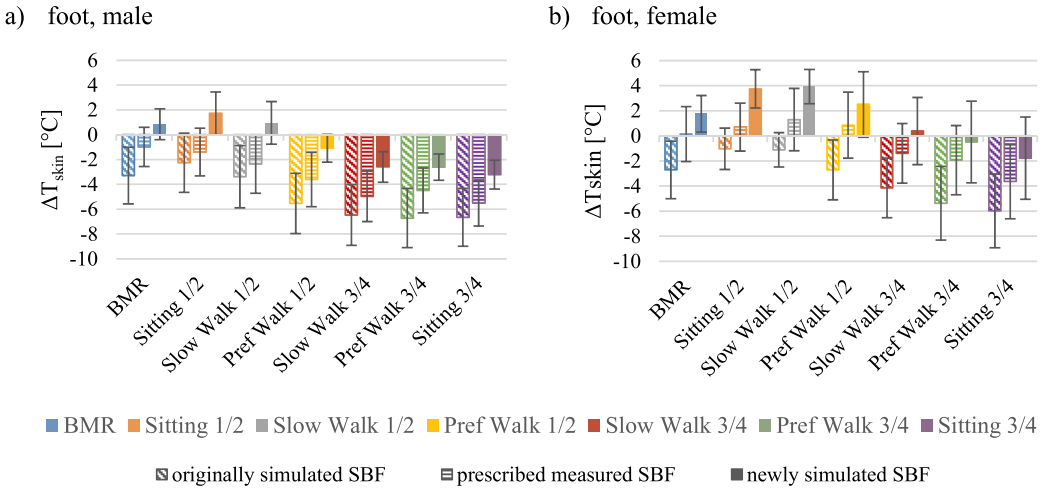

Fig. 11. Comparison of foot skin temperature differences for male and female subjects (simulated - measured) using the originally simulated SBF (equation (2)) versus the newly simulated (equation (5)) SBF.

overestimated by $1.5 - 4°C$ in the first sitting, slow walking and preferred walking sessions. This observation can already be seen for the results using the prescribed measured SBF, but is now more pronounced, which might be due to the exclusion of subjects and the regression method.

4. Discussion

The results showed that the prediction of local skin temperatures by a thermophysiological model could be improved for higher activity levels, if the neurophysiological SBF model includes the activity level and gender of the subjects. For the most accurate prediction of SBF, the model might be extended by further factors such as blood pressure, hormonal changes or local muscle activity levels (Kingma et al., 2014). At the current stage these factors are indirectly included in the constant γ_1 of the neurophysiological model (see equation (2) and equation (4)). However, it is important to weigh the contribution to accuracy of a variable against the effort it takes and the possibility to obtain it. For example, the whole simulation model would probably benefit from measurements of local muscular heat production due to activity e.g. using EMG. However, even though this value might be measured in the laboratory, users of the simulation model might not be able to access the data. In contrast, the estimation of the whole-body activity level is well-document in the literature and standards (EN-ISO 8996, 2004; Parsons, 2014). In future research, an indirect method, e.g. measuring local blood perfusion and local skin temperatures and a detailed heat transfer model might be used to reconstruct the local metabolic rates. An alternative implementation would be that the neurophysiological model is maintained in pure form and then a unique set of weights on the afferent neurophysiological input is required based on the activity pattern (i.e. a table of weights based on *act*).

The skin temperature predictions for the foot showed the largest ΔT_{skin} and standard deviation of all body parts of up to $6.0 \pm 2.4°C$. Furthermore, ΔT_{skin} was up to $4.5°C$ different for morning and afternoon sessions of the same activity. Both effects were most dominant in the original simulation, but could still be seen when the simulation was run with the measured SBF or the new neural signal equation for foot SBF. This observation might suggest that the large deviation was not only due to a simulation inaccuracy, but also due to a systematic effect or an error in measurement. In the study by van Marken Lichtenbelt et al. (2007), which validated an earlier version of an individualized ThermoSEM model for male subjects lying in a neutral and mildly cold environment, the mean skin temperature difference at the foot and hand was reported to be the highest compared to other body parts with the foot skin temperature being $2.5°C$ or less. Hence, it could be expected that $\Delta T_{skin,foot}$ is slightly higher than ΔT_{skin} at other body parts. However, this reasoning does not explain the change in $\Delta T_{skin,foot}$ between morning and afternoon sessions. For the difference between morning and afternoon session, the effect of circadian rhythm may have played role. Kräuchi et al., 1999; Kräuchi and Wirz-Justice, 1994 and van Marken Lichtenbelt et al. (2006) showed that distal skin temperatures can vary between $1\ °C$ to $5°C$ during the course of a 24-h period. However, in the time period of our experiments, which was from about 8:30 to 14:00 h, the variations were lower at $0.5°C$ at maximum for $\Delta T_{skin,foot}$ (Kräuchi and Wirz-Justice, 1994) Also, the difference in $\Delta T_{skin,loc}$ between the morning and afternoon sessions was less than $1°C$ for all other body parts. Hence, the effect of circadian rhythm might only have had a minor part of the differences in $\Delta T_{skin,foot}$ of the morning and afternoon session. Another reason could be that the thermal properties of some shoes of the participants did not match the measured (average) thermal properties which were included in the thermophysiological model's input parameters. Shoes with higher dry and evaporative resistance values could lead to heat and sweat accumulation in the shoes, causing the temperature to rise over time (Gavin, 2003; Kuklane et al., 1999). Also, the swelling of the feet or legs after longer periods of sitting or wearing footwear might play a role (Kristjuhan, 1995). Due to this tissue swelling, the blood perfusion would be hindered resulting in different skin temperatures between the morning and afternoon sessions. However, this assumption is not supported by the SBF measurements as shown in Fig. 7 which are very similar for the morning and afternoon session. Hence, future studies may consider that participants take off shoes during breaks, to reduce heat accumulation. Standardized footwear might also be an option to this issue, but could be too costly because of the variety of shoe sizes and may not provide a suitable fit and comfort to the participants.

The foot skin temperature was not only affected by foot SBF, but also by total blood flow into the foot (warming from the foot core). Thus, plethysmography would have been another method to cover the total blood flow, since it measures the total blood flow in the deep layer tissues and in the superficial tissue layer. However, exercise would have to be interrupted for that. The blood flow in the deeper tissue layers is generally related to the metabolic functions of the extremity and has a constant and modest blood flow (Lotens, 1989). In the extremities most effects are caused by the change in the SBF, which can be measured by LDF. The blood flow in the deeper tissue layers was not directly measured but included in the ThermoSEM model. The effects of (partly) cooling by other body parts on the core temperature of the feet ($T_{c,foot}$) is taken into account by the counter current heat exchange coefficients

(CCX) in the ThermoSEM model. The warming from the foot core depends on $T_{c,foot}$ and the thermal insulation of its surrounding tissue, which is affected by the local skin perfusion.

To avoid the artefacts in the LDF signal during walking, the LDF data was evaluated for the 3 min directly after the subjects stopped moving. In Snell et al. (1987), the leg SBF was relatively constant for the recorded 2: 20 *min* after the prescribed exercise with a peak at about 1 min after the exercise. Hence, we assumed that the mean of the LDF signal of the 3 min gives a sufficient estimate for the foot SBF. Also, the small breaks during an activity where designed to be about 3–4 min, to avoid a large changes in energy expenditure and SBF. In some cases, these small breaks were shorter or had error values, due to adjustments of the probe. For these occurrences, a shorter period of stable LDF signal was evaluated. For future studies, a second probe on the other foot and more repetitions of the same session, could improve the interpretation of the LDF signal.

In the literature, no direct comparison for the increase in ankle SBF due to walking at moderate speeds was found. In the studies by Hinds et al. (2004), Joyner et al. (2001), Savard et al. (1988) and Snell et al. (1987), the increase in leg SBF was between 20 and 50-fold compared to a resting scenario. However, the level of exercise was with 80–100% of the subjects' leg maximal performance capacity much higher compared to the slow and preferred walking scenario of this study. Hence, a mean 3-5-fold increase in foot SBF seems to in reasonable relation, especially since Joyner et al. (2001) show a more steep increase in SBF with elevated walking speeds.

In this study, the variances in the measured foot SBF were very large (Fig. 7). To some extent, the range of participants' characteristics might have caused these variations. Also, local basal SBF changed due to a circadian and ultradian rhythm of the course of 24 h (Yosipovitch et al., 2004). Since this effect might be overshadowed by the prescribed activities, it most likely only has had a minor effect of the foot SBF during walking. Three main reasons can be identified that might have caused the high variances and influenced the results. Firstly, the menstrual phase of the female subjects during the experiments were not considered due to organizational reasons. Bartelink et al. (1990) show that the peripheral perfusion changes significantly during the menstrual cycle, which also cause significant skin temperature differences in the same environmental conditions. Hence, this might be one of the reasons for the larger variance in females than males for the measured foot SBF. Secondly, the study by Snell et al. (1987) showed a significant difference in maximal leg SBF for untrained and trained participants. When recruiting the subjects for our study, this aspect was not considered. The statue and background of the subjects (e.g. daily use of bicycle) may suggest slight difference in fitness. Hence, some variation might due to this issue. Thirdly, even though the experimenters paid great attention to the fixation of the probes, it is possible that the LDF probe on the ankle became looser during the walking session, causing measurement artefacts. Because of the walking movement, the probe was exposed to higher forces than for measurements at seated or lying postures. These issues on the high variance in SBF might be reduced in future studies by using a second probe on the other foot or other measured body part, and more repetitions of the same session with adjusting the probe in between.

Another difference between male and female subjects can be seen in the increase of the ratios of mean normalized, measured SBF and mean normalized, simulated SBF of the foot. For males, the values varied from 1.8 to 4.2 and for females from 4.5 to 7.9. This observation raises the question on whether the smaller change in males is due their generally higher foot skin temperature (about $0.8°C$ for this study) and higher absolute SBF. Local foot temperatures will affect the (local) thermoregulatory responses and therefore, the SBF (Brengelmann and Savage, 1997). However, it is not clear to what extend this can explain all these differences or if other effects also play a role.

For all simulations and participants in this study, the core temperature was underestimated by $1.2°C - 1.3°C$ on average (Fig. 9). There was a slight increase in core temperature difference due to the implementation of the measured SBF compared to the simulated SBF of $0.05°C$. In general, the values were larger than could be excepted from the accuracy of the CorTemp pill of $\pm$ $0.27°C$(Bongers et al., 2018). One reason for the relatively large core temperature difference was found in the individualization of ThermoSEM (subjects' geometry), which accounts for approximately $0.7°C$. This effect might be due to the fact that the model was developed for an average male human, and parameters, such as the basal blood perfusion rate, are scaled with the volume of the body parts. Probably, the scaling should not only be based one-to-one with the geometry, but corrected by some unknown factor. Kingma et al. (2014) also identified the counter current heat exchange as a source for deviations in core temperature. In their study, increased counter current heat exchange coefficients led to a higher core temperature by $0.2°C$. Moreover, Kräuchi et al., 1999, Kräuchi and Wirz-Justice, 1994 showed that the core temperature changes during a 24-h period (circadian effect). The difference in core temperature between 8 o'clock and 14 o'clock was about $0.4°C$ for resting subjects. In contrast, this study considered active participants. The influence of activity on the core temperature might exceed the influence of the circadian effect. Hence, the influence of the circadian effect on the core skin temperature difference cannot be quantified. In summary, further research on the physiological individualization of ThermoSEM and on counter current heat exchange is needed to provide further improvement of the core temperature prediction.

The new neurophysiological model of the foot SBF mostly led to improved foot skin temperature prediction. This result is promising for developing an extended set of new neural regulation signal equations that include activity levels above 1 *met* and gender differences in SBF, especially since the largest deviations in ΔT_{skin} were seen for this body part. In future research, the SBF measurements should be extended to additional body sites, especially at upper and lower extremities, since they are part of the moving process. Additionally, one or two locations at the torso might be included for comparison to the SBF of the neurophysiological model by Kingma et al. (2014).

In this study, the measurements were performed at a uniform and constant ambient temperature ($T = 24°C$), at activity levels in the range $1 - 3$ *met* (sitting – walking) and subjects wearing light and medium clothing ensembles including sneakers. In contrast, the original neurophysiological model was developed on a measurement protocol which included temperature changes, but only in supine position and with low clothing insulation and only socks instead of shoes (Kingma et al., 2014). To have a complete adjusted neurophysiological model, future research could also include a combination of increased activity levels and different ambient temperatures.

Overall, although some issues have been raised, the results showed that by including the walking activity level and gender in the neural signal model for the skin blood flow, the local skin temperatures can be predicted more accurately. Ideally, the improvements implemented through future studies will predict individual local skin temperatures within the error of the skin temperatures measurement (e.g. with iButtons), which would practically be $\pm$ $1°C$ (van Marken Lichtenbelt et al., 2006). At the current stage, individual results were deviating from this aim by up to 6 $°C$ for the feet and up to $4°C$ for all other body parts. However, the average was much closer to the ideal value. Hence, the current version including the improved neurophysiological model of the foot would be applicable to a group of people rather than to individuals, which is the case, for example, in the built environment.

Apart from applications in the built environment, an advanced thermophysiological model including a precise SBF model might also be applied to other research areas of human physiology such as sport science and medical purposes. In sport science, a thermoregulation model might be used to investigate athletes' heat stress before a training unit or competition (Havenith, 2001; Havenith and Fiala, 2016). The use of precooling or percooling can reduce this heat stress and improve performance (Bongers et al., 2015; Eijsvogels et al., 2014; Luomala

et al., 2012). A thermophysiological model can be used to preselect promising cooling strategies, without the time and monetary investment of human subject experiments. In medicine, the prediction and observation of a patient's temperature can be critical for the success of medical surgeries. The studies by Droog et al. (2012) and Severens et al. (2007) give examples of applying a thermophysiological model to the human temperature management during kidney dialysis and open-heart surgery, respectively.

5. Conclusions

The accuracy of local skin temperature and local thermal sensation prediction using human thermophysiological models largely depends on the precision of their local heat balances. Local skin blood flow is a major part of these balances. This study reveals that the skin blood flow and local skin temperature prediction using current neurophysiological model can be improved when walking activity levels above 1 met and gender differences are included in the neurophysiological model. A precise thermophysiological model including accurate skin blood flow prediction can help to optimize the energy consumption and thermal comfort in the built environment. Additionally, it might be applied to other research areas in human physiology such as sport science and patient's temperature management.

Funding

The study received funding from TKI Energo and TKI Solar Energy (TEGB|13023).

Compliance with ethical standards

Conflicts of interest

The authors declare that they have no conflict of interest.

Ethical approval

All procedures performed in studies involving human participants were in accordance with the ethical standards of the institutional and/or national research committee and with the 1964 Helsinki declaration and its later amendments or comparable ethical standards.

Informed consent

Informed consent was obtained from all individual participants included in the study.

Acknowledgements

The authors like to thank the participants of this study for their time and cooperation. A special thank also to the technical and scientific staff of Maastricht University that made this study possible. Furthermore, we would like to thank TKI Energo and TKI Solar Energy for the received funding (TEGB|13023).

Appendix A. Supplementary data

Supplementary data to this article can be found online at https://doi.org/10.1016/j.jtherbio.2019.07.033.

References

Arens, E., Bauman, F., Johnston, L.P., Zhang, H., 1991. Testing of localized ventilation systems in a new controlled environment chamber. Indoor Air 1, 263–281.

Bartelink, M.L., Wollersheim, H., Theeuwes, A., van Duren, D., Thien, T., 1990. Changes in skin blood flow during the menstrual cycle: the influence of the menstrual cycle on the peripheral circulation in healthy female volunteers. Clin. Sci. (Lond.) 78, 527–532. https://doi.org/10.1042/CS0780527.

Bongers, C.C.W.G., Daanen, H.A.M., Bogerd, C.P., Hopman, M.T.E., Eijsvogels, T.M.H., 2018. Validity, reliability, and inertia of four different temperature capsule systems. Med. Sci. Sport. Exerc. 50, 169–175. https://doi.org/10.1249/MSS.0000000000001403.

Bongers, C.C.W.G., Thijssen, D.H.J., Veltmeijer, M.T.W., Hopman, M.T.E., Eijsvogels, T.M.H., 2015. Precooling and percooling (cooling during exercise) both improve performance in the heat: a meta-analytical review. Br. J. Sports Med. 49, 377–384. https://doi.org/10.1136/bjsports-2013-092928.

Boulant, J.A., 2005. Neuronal basis of Hammel's model for set-point thermoregulation. J. Appl. Physiol. 100, 1347–1354. https://doi.org/10.1152/japplphysiol.01064.2005.

Brengelmann, G.L., Savage, M.V., 1997. Temperature regulation in the neutral zone. Ann. N. Y. Acad. Sci. 813, 39–50. https://doi.org/10.1111/j.1749-6632.1997.tb51670.x.

Droog, R.P.J., Kingma, B.R.M., van Marken Lichtenbelt, W.D., Kooman, J.P., van der Sande, F.M., Levin, N.W., van Steenhoven, A.A., Frijns, A.J.H., 2012. Mathematical modeling of thermal and circulatory effects during hemodialysis. Artif. Organs 36, 797–811. https://doi.org/10.1111/j.1525-1594.2012.01464.x.

Du Bois, D., Du Bois, E.F., 1916. A formula to estimate the approximate surface area if height and weight be known. Arch. Intern. Med. XVII 863–871.

Eijsvogels, T.M.H., Bongers, C.C.W.G., Veltmeijer, M.T.W., Moen, M.H., Hopman, M., 2014. Cooling during exercise in temperate conditions: impact on performance and thermoregulation. Int. J. Sports Med. 35, 840–846. https://doi.org/10.1055/s-0034-1368723.

EN-ISO 8996, 2004. EN-ISO 8996, Ergonomics of the Thermal Environment - Determination of Metabolic Heat Production.

EN-ISO 9886, 2004. Ergonomics - Evaluation of Thermal Strain by Physiological Measurements.

Fiala, D., 1998. Dynamic Simulation of Human Heat Transfer and Thermal Comfort. Dissertation. De Montfort University, Leicester.

Fiala, D., Havenith, G., Bröde, P., Kampmann, B., Jendritzky, G., 2012. UTCI-Fiala multi-node model of human heat transfer and temperature regulation. Int. J. Biometeorol. 56, 429–441.

Fiala, D., Lomas, K.J., Stohrer, M., 2001. Computer prediction of human thermoregulatory and temperature responses to a wide range of environmental conditions. Int. J. Biometeorol. 45, 143–159.

Fiala, D., Lomas, K.J., Stohrer, M., 1999. A computer model of human thermoregulation for a wide range of environmental conditions: the passive system. J. Appl. Physiol. 87, 1957–1972.

Foda, E., Sirén, K., 2012. Design strategy for maximizing the energy-efficiency of a localized floor-heating system using a thermal manikin with human thermoregulatory control. Energy Build. 51, 111–121.

Gavin, T.P., 2003. Clothing and thermoregulation during exercise. Sport. Med. 33, 941. https://doi.org/10.1159/000072236.

Havenith, G., 2001. Individualized model of human thermoregulation for the simulation of heat stress response. J. Appl. Physiol. 90, 1943–1954.

Havenith, G., Fiala, D., 2016. Thermal indices and thermophysiological modeling for heat stress. Comp. Physiol. 6, 255–302. https://doi.org/10.1002/cphy.c140051.

Hinds, T., McEwan, I., Perkes, J., Dawson, E., Ball, D., George, K., 2004. Effects of massage on limb and skin blood flow after quadriceps exercise. Med. Sci. Sport. Exerc. 36, 1308–1313. https://doi.org/10.1249/01.MSS.0000135789.47716.DB.

Huizenga, C., Zhang, H., Arens, E., 2001. A model of human physiology and comfort for assessing complex thermal environments. Build. Environ. 36, 691–699.

IEA, 2013. Transition to Sustainable Buildings. Paris, France.

ISO 9920, 2009. Ergonomics of the Thermal Environment - Estimation of Thermal Insulation and Water Vapour Resistance of a Clothing Ensemble.

Joyner, M.J., Dietz, N.M., Shepherd, J.T., 2001. From Belfast to Mayo and beyond: the use and future of plethysmography to study blood flow in human limbs. J. Appl. Physiol. 91, 2431–2441.

Kellogg, D.L., 2006. In vivo mechanisms of cutaneous vasodilation and vasoconstriction in humans during thermoregulatory challenges. J. Appl. Physiol. 100, 1709–1718. https://doi.org/10.1152/japplphysiol.01071.

Kingma, B.R.M., 2012. Human Thermoregulation: a Synergy between Physiology and Mathematical Modelling. Dissertation. Maastricht University.

Kingma, B.R.M., Vosselman, M.J., Frijns, A.J.H., Van Steenhoven, A. a., van Marken Lichtenbelt, W.D., 2014. Incorporating neurophysiological concepts in mathematical thermoregulation models. Int. J. Biometeorol. 58, 87–99.

Kirkpatrick, P.J., Smielewski, P., Czosnyka, M., Pickard, J.D., 1994. Continuous monitoring of cortical perfusion by laser Doppler flowmetry in ventilated patients with head injury. J. Neurol. Neurosurg. Psychiatry 57, 1382–1388. https://doi.org/10.1136/jnnp.57.11.1382.

Kräuchi, K., Cajochen, C., Werth, E., Wirz-Justice, A., 1999. Warm feet promote the rapid onset of sleep. Nature 401, 36–37.

Kräuchi, K., Wirz-Justice, A., 1994. Circadian rhythm of heat production, heart rate, and skin and core temperature under unmasking conditions in men. Am. J. Physiol. Integr. Comp. Physiol. 267, R819–R829. https://doi.org/10.1152/ajpregu.1994.267.3.r819.

Kristjuhan, Û., 1995. Arm and leg girths of industrial workers during a workday. Int. J. Occup. Saf. Ergon. 1, 193–198. https://doi.org/10.1080/10803548.1995.11076317.

Kuklane, K., Holmer, I., Giesbrecht, G., 1999. Change of footwear insulation at various sweating rates. Appl. Hum. Sci. J. Physiol. Anthropol. 18, 161–168. https://doi.org/10.2114/jpa.18.161.

Lotens, W.A., 1989. A Simple Model for Foot Temperature Simulation. IZF 1989-8. TNO Institute for Perception, Soesterberg.

Luomala, M.J., Oksa, J., Salmi, J.A., Linnamo, V., Holmér, I., Smolander, J., Dugué, B., 2012. Adding a cooling vest during cycling improves performance in warm and

humid conditions. J. Therm. Biol. 37, 47–55. https://doi.org/10.1016/j.jtherbio.2011.10.009.
Martínez, N., Quesada, J.I.P., Corberán, J.M., de Anda, R.M.C.O., Kuklane, K., Palmer, R.S., Soriano, P.P., Psikuta, A., Rossi, R.M., Annaheim, S., 2016. Validation of the thermophysiological model by Fiala for prediction of local skin temperatures. Int. J. Biometeorol. 60, 1969–1982. https://doi.org/10.1007/s00484-016-1184-1.
Mekjavič, I., Morrison, J.B., 1985. A model of shivering thermogenesis based on the neurophysiology of thermoreception. IEEE Trans. Biomed. Eng. 32, 407–417.
Melikov, A.K., Arakelian, R.S., Halkjaer, L., Fanger, P.O., 1994. Spot cooling. Part 2: recommendations for design of spot-cooling systems. ASHRAE Transact. 100, 500–510.
Nakamura, K., Morrison, S.F., 2008a. Preoptic mechanism for cold-defensive responses to skin cooling. J. Physiol. 586, 2611–2620. https://doi.org/10.1113/jphysiol.2008.152686.
Nakamura, K., Morrison, S.F., 2008b. A thermosensory pathway that controls body temperature. Nat. Neurosci. 11, 62–71.
Parsons, K.C., 2014. Human Thermal Environments: the Effects of Hot, Moderate, and Cold Environments on Human Health, Comfort, and Performance, third ed. ed. CRC Press.
Pennes, H.H., 1948. Analysis of tissue and arterial blood temperatures in the resting human forearm. J. Appl. Physiol. 1, 93–122.
Psikuta, A., Fiala, D., Laschewski, G., Jendritzky, G., Richards, M., Błażejczyk, K., Mekjavič, I., Rintamäki, H., de Dear, R.J., Havenith, G., 2012. Validation of the Fiala multi-node thermophysiological model for UTCI application. Int. J. Biometeorol. 56, 443–460.
Savard, G.K., Nielsen, B., Laszczynska, J., Larsen, B.E., Saltin, B., 1988. Muscle blood flow is not reduced in humans during moderate exercise and heat stress. J. Appl. Physiol. 64, 649–657. https://doi.org/10.1152/jappl.1988.64.2.649.
Schellen, L., Loomans, M.G.L.C., Kingma, B.R.M., de Wit, M.H., Frijns, A.J.H., van Marken Lichtenbelt, W.D., 2013. The use of a thermophysiological model in the built environment to predict thermal sensation. Build. Environ. 59, 10–22.
Severens, N.M.W., 2008. Modelling Hypothermia in Patients Undergoing Surgery. Dissertation. Eindhoven University of Technology.
Severens, N.M.W., van Marken Lichtenbelt, W.D., Frijns, A.J.H., van Steenhoven, A.A., De Mol, B.A.J.M., Sessler, D.I., 2007. A model to predict patient temperature during cardiac surgery. Phys. Med. Biol. 52, 5131–5145.
Snell, P.G., Martin, W.H., Buckey, J.C., Blomqvist, C.G., 1987. Maximal vascular leg conductance in trained and untrained men. J. Appl. Physiol. 62, 606–610. https://doi.org/10.1152/jappl.1987.62.2.606.
Tanabe, S.I., Kobayashi, K., Nakano, J., Ozeki, Y., Konishi, M., 2002. Evaluation of thermal comfort using combined multi-node thermoregulation (65MN) and radiation models and computational fluid dynamics (CFD). Energy Build. 34, 637–646.
van Marken Lichtenbelt, W.D., Daanen, H. a M., Wouters, L., Fronczek, R., Raymann, R.J.E.M., Severens, N.M.W., Van Someren, E.J.W., 2006. Evaluation of wireless determination of skin temperature using iButtons. Physiol. Behav. 88, 489–497.
van Marken Lichtenbelt, W.D., Frijns, A.J.H., Fiala, D., Janssen, F.E.M., van Ooijen, A.M.J., Van Steenhoven, A.A., 2004. Effect of individual characteristics on a mathematical model of human thermoregulation. J. Therm. Biol. 29, 577–581.
van Marken Lichtenbelt, W.D., Frijns, A.J.H., Van Ooijen, M.J., Fiala, D., Kester, A.M., Van Steenhoven, A. a., 2007. Validation of an individualised model of human thermoregulation for predicting responses to cold air. Int. J. Biometeorol. 51, 169–179.
Verhaart, J., Veselý, M., Zeiler, W., 2015. Personal heating: effectiveness and energy use. Build. Res. Inf. 43, 346–354. https://doi.org/10.1080/09613218.2015.1001606.
Veselá, S., Kingma, B.R.M., Frijns, A.J.H., 2017a. Local thermal sensation modeling-a review on the necessity and availability of local clothing properties and local metabolic heat production. Indoor Air 27, 216–272.
Veselá, S., Kingma, B.R.M., Frijns, A.J.H., 2015. Taking thermal regulation models from the lab to the world: are current views ready for the challenge? In: Loomans, M.G.L.C., te Kulve, M. (Eds.), Healthy Buildings Europe 2015. Eindhoven.
Veselá, S., Psikuta, A., Frijns, A.J.H., 2018. Local clothing thermal properties of typical office ensembles under realistic static and dynamic conditions. Int. J. Biometeorol. 62, 2215–2229. https://doi.org/10.1007/s00484-018-1625-0.
Veselá, S., Psikuta, A., Kingma, B.R.M., Frijns, A.J.H., 2017b. Measurements of local clothing resistances and local area factors under various conditions. In: Healthy Buildings 2017 Europe. Lublin, Poland.
Veselý, M., Zeiler, W., 2014. Personalized conditioning and its impact on thermal comfort and energy performance - a review. Renew. Sustain. Energy Rev. 34, 401–408.
Wissler, E.H., 2008. A quantitative assessment of skin blood flow in humans. Eur. J. Appl. Physiol. 104, 145–157. https://doi.org/10.1007/s00421-008-0697-7.
Wölki, D., 2017. MORPHEUS : Modelica-Based Implementation of a Numerical Human Model Involving Individual Human Aspects. RWTH Aachen University, Aachen.
Wölki, D., van Treeck, C., 2013. Individualization of a mathematical manikin model in terms of gender, age and morphological issues for predicting thermal comfort: a preliminary study. In: Wurtz, E. (Ed.), BS 2013 : 13th International Conference of the International Building Performance Simulation Association, August 26-28. Chambery, France, pp. 1649–1656.
Yosipovitch, G., Sackett-Lundeen, L., Goon, A., Huak, C.Y., Goh, C.L., Haus, E., 2004. Circadian and ultradian (12 h) variations of skin blood flow and barrier function in non-irritated and irritated skin - effect of topical corticosteroids. J. Investig. Dermatol. 122, 824–829. https://doi.org/10.1111/j.0022-202X.2004.22313.x.
Zhang, H., Huizenga, C., Arens, E., Yu, T., 2001. Considering individual physiological differences in a human thermal model. J. Therm. Biol. 26, 401–408.